J. Biochem. 2011;149(5):609–618 doi:10.1093/jb/mvr010

JB THE JOURNAL OF BIOCHEMISTRY

Single molecule imaging of the *trans*-translation entry process via anchoring of the tagged ribosome

Received December 29, 2010; accepted January 17, 2011; published online January 28, 2011

Zhan-Ping Zhou[1], Yoshihiro Shimizu[1], Hisashi Tadakuma[1,*], Hideki Taguchi[2], Koichi Ito[3] and Takuya Ueda[1]

[1]Graduate School of Frontier Science, The University of Tokyo, 5-1-5 Kashiwanoha, Kashiwa-shi, Chiba 277-8562; [2]Graduate School of Bioscience and Biotechnology, Tokyo Institute of Technology, Kanagawa 226-8501, Japan; and [3]Institute of Medical Science, The University of Tokyo, Tokyo 108-8639, Japan

*Hisashi Tadakuma, Graduate School of Frontier Science, The University of Tokyo, 5-1-5 Kashiwanoha, Kashiwa-shi, Chiba 277-8562, Japan. Tel: +81-4-7136-3648, Fax: +81-4-7136-3648, email: tadakuma@molbio.t.u-tokyo.ac.jp

***Trans*-translation is an eubacterial quality control system to rescue the stalled ribosome, in which multiple components such as transfer messenger RNA (tmRNA) and Small protein B (SmpB) are involved. However, how these molecules interact with ribosome remains elusive. Here, we report the single molecule analysis of the *trans*-translation process. We developed a new method to label the functional ribosome, in which a tag protein (the HaloTag protein of 297 amino acids) was fused to the 30S ribosomal protein S2 and covalently labelled with specific ligand (HaloTag ligand), resulting in the stable and specific labelling of ribosome. Ribosomes were anchored onto the glass surface using biotinylated derivative of the Cy3 HaloTag ligand (*i.e.* biotin–Cy3–ligand), and real-time interactions of Cy5–tmRNA/SmpB/EF–Tu ternary complexes with anchored ribosomes are observed as a model of the *trans*-translation entry. Statistical analysis revealed that Cy5–tmRNA/SmpB/EF–Tu ternary complexes bind to the anchored ribosome with the second-order rate constant of 2.6×10^6 (1/M/s) and tmRNAs undergo multi-modal pathway before release from ribosome. The methods presented here are also applicable to the analysis for general translation processes.**

Keywords: HaloTag/single molecule/ribosome/*trans*-translation/tmRNA.

Abbreviations: MLD, mRNA-like domain; PEG, polyethylene glycol; PMB, poly [2-methacryloyloxyethyl phosphorylcholine (MPC)–co–*n*-butyl methacrylate (BMA)]; SmpB, Small protein B; TLD, tRNA-like domain; TMR, tetramethylrhodamine.

In eubacteria, stalled translating ribosomes on defective mRNA templates are rescued by the *trans*-translation system, a unique protein quality control system facilitated by transfer messenger RNA (tmRNA) and Small protein B (SmpB). The tmRNA, which is composed of a tRNA-like domain (TLD), an mRNA-like domain (MLD) and four pseudoknots, plays multiple roles at three key steps of *trans*-translation, *i.e.* entry, elongation and termination steps. At the entry step, alanine-charged tmRNA, together with SmpB and EF–Tu (*i.e.* tmRNA/SmpB/EF–Tu ternary complex), acts as tRNA. After entry, swapping of the defective mRNA to MLD takes place. The elongation process then resumes using MLD as the template, and a short degradation tag peptide (the SsrA peptide of 11 amino acids) is added to the nascent stalled peptide. Finally, this peptide is released using tmRNA containing termination codons.

Recent progress has revealed many aspects of *trans*-translation (*1*, *2*). However, its detailed molecular mechanism remains elusive. One reason is the complexity of the *trans*-translation process. In a conventional biochemical assay, it is important to synchronize the process to avoid hindrance by ensemble averaging. But the multi-step process of *trans*-translation makes it difficult to synchronize the whole process. In contrast, single molecule techniques have an advantage for understanding such multi-step biological processes, as the obtained data are not obscured by ensemble averaging. Thus, single molecule techniques might be a powerful tool to elucidate the precise mechanism of *trans*-translation.

In previous reports on single molecule imaging of the normal translation process, the association of tRNA or the structural change of the ribosome was monitored (*3*–*7*) by anchoring active ribosome complexes on a glass surface via template (mRNA) anchoring. This method is thought to be inappropriate for the observation of ribosomes in *trans*-translation, however, since the mRNA is supposed to be released from the stalled ribosome complex at an early stage of the process. Thus, an alternative method other than mRNA anchoring is required. Puglisi and colleagues (*8*, *9*) reported a convenient method, in which the modified ribosome with an extended loop moiety is directly anchored via antisense DNA fixed on the glass surface. But the non-covalent interaction between the extended loop RNA and the antisense DNA, unfortunately, was shown to be insufficient to stably hold the translating ribosome during the entire *trans*-translation process (data not shown). The other method is to modify the 3′-end of 23S rRNA (by periodate oxidation) with subsequent conjugation of chemical moieties such as biotin (*10*). This method provides a much more stable interaction between ribosomes and the glass surface than the oligo DNA method. But, the non-specific

labelling of biotin to other 50S components (such as 5S RNA) might occur.

Here, we propose a new method to overcome these drawbacks, *i.e.* insufficient anchoring strength and non-specific labelling. In our approach, the wild-type *Escherichia coli* ribosomal protein S2 gene (*rpsB*) was replaced with a HaloTag-engineered variant in such a way so as not to disturb the S2 function or normal cell growth, and the co-biosynthetically tagged ribosome was purified. The HaloTag protein is a commercially available small protein (297 amino acids; MW 34 kDa, Promega) derived from haloalkane dehalogenase, which can specifically form covalent bonds *in vitro* and *in vivo* with designed aliphatic halogenated ligands that are conjugated with various chemical moieties for diverse purposes such as fluorescent dye labels, affinity handles and attachments to a solid phase. Therefore, this feature provides the HaloTagged ribosome with a unique platform for a variety of modifications such as fluorescent labelling and/or anchoring on the glass surface.

In this study, using the advantage of tagged ribosomes, we were able to stably anchor ribosomes on quartz slides. As a first step in observing the *trans*-translation, we measured the specific interaction of the tmRNA/SmpB/EF–Tu ternary complex on a ribosome. Single molecule experiments revealed the multi-associative mode of the Cy5–tmRNA/SmpB/EF–Tu ternary complex, showing the potential of a single molecule study in elucidating the *trans*-translation mechanism. Our method provides a basis for *trans*-translation imaging and a simple, rapid and specific way to obtain labelled ribosomes *in vitro* and *in vivo*.

Materials and Methods

Preparation of fluorescently labelled tagged ribosomes

Ribosomes were prepared according to Ohashi *et al.* (*11*). The HaloTag protein coding sequence was attached to the intact wild-type rpsB gene with linker sequences. Details of the construction of the tagged ribosome will be published elsewhere (H. Tadakuma *et al.*, manuscript in preparation). Purified ribosomes were finally dissolved in 70S buffer [20 mM HEPES–KOH (pH 7.6), 6 mM $Mg(OAc)_2$, 30 mM KCl and 7 mM β-mercaptoethanol] and divided small aliquots were frozen in liquid nitrogen and stored at −80°C until use. The final yield of ribosomes from 1 l culture was estimated to be 10 nmol (20 μM × 0.5 ml). To obtain tetramethylrhodamine (TMR)-labelled ribosomes, ribosomes were incubated with fluorescently conjugated HaloTag ligand (TMR–HaloTag ligand; Promega) at a molar ratio of 1 : 4 in 70S buffer for 30 min at room temperature. Unreacted dye was removed by gel filtration (MicroSpin S300 HR, GE). Using spectrophotometer (V-550; Jasco), the labelling ratio was estimated to be 0.9 TMR–dye/ribosome, assuming that the molar absorbance coefficient was $\varepsilon 260 = 41.7 \times 10^6\,M^{-1}\,cm^{-1}$ for ribosomes and $\varepsilon 550 = 95{,}000\,M^{-1}\,cm^{-1}$ for TMR. In contrast, the non-specific labelling ratio of intact wild-type ribosomes was less than 0.01 TMR/ribosome. The biotinylated derivative of the Cy3–HaloTag ligand (biotin–Cy3–HaloTag ligand) used for anchoring was synthesized as reported previously (*12*, *13*). Briefly, Cy3 bis-Reactive Dye (PA23,000, GE) in DMSO were mixed with HaloTag Amine (O4) Ligand (P6741, Promega) in the presence of excess Triethylamine (208–02643, Wako) and incubated at 50°C, then Biotin–(AC5)2–hydrazide (341–06421, Dojindo) and additional Triethylamine were added to the reaction mixture and incubated further. The labelling ratio of Cy3 was estimated from the absorbance at 260 and 550 nm, assuming a molar absorbance coefficient of $\varepsilon 260 = 41.7 \times 10^6\,M^{-1}\,cm^{-1}$ and $\varepsilon 550 = 150{,}000\,M^{-1}\,cm^{-1}$ for the ribosomes and Cy3, respectively. The labelling efficiency was estimated to be 60%. The low labelling efficiency compared with the TMR ligand might have been caused by the omission of the purification step, *i.e.* separation of the active from the unreactive ligand. Biotinylation of the biotin–Cy3–ligand-labelled ribosome was confirmed using the FluoReporter Biotin Quantitation Assay Kit (F30751, Invitrogen) and estimated to be at least 15%. To confirm the incorporation of S2–Halo into the ribosomes, 10 pmol of TMR-labelled samples was applied to a 12% SDS–PAGE gel, and the TMR image was captured by a photo-imager (LAS4,000; FUJIFILM). The gel was further stained with SYPRO Orange (S6650, Invitrogen) to detect the protein, and the image was captured by a photo-imager. For the sucrose density gradient centrifugation (SDG) experiment presented in Fig. 1, 100 pmol of samples (2 μM × 50 μl) was applied onto a 20–50% (w/v) sucrose gradient, and centrifuged at 210,000*g* for 7 h with a SW41Ti rotor (Beckman Coulter).

Labelling of tmRNA

Escherichia coli tmRNA was transcribed *in vitro* as described previously (*14*). Then the guanine residues of the tmRNAs were randomly labelled using a Cy5 labelling kit (Label IT; Mirus) and unreacted dye was removed by ethanol precipitation (*15*). The efficiency of Cy5 labelling of the tmRNA was calculated from the absorbance of tmRNA at 260 nm and Cy5 at 650 nm, assuming molar absorbance coefficients of 3.1×10^6 (tmRNA) and 0.25×10^6 (Cy5). Depending on the purpose of each experiment, the labelling ratio was modified by changing the molar ratio of tmRNA to Cy5 dye. Samples with a low labelling ratio (1 Cy5/tmRNA) were used for single molecule observation and samples with 3 Cy5/tmRNA were used for SDG, GTPase measurements and SsrA-tagging assay. The fluorescent samples were stored at −80°C until use. For the SDG illustrated in Fig. 2, 100 μl of samples was layered onto a 20–50% (w/v) sucrose gradient, and ultracentrifuged at 222,000*g* for 16 h with a SW41Ti rotor (Beckman Coulter).

Measurement of the GTPase activity of EF–Tu

The ribosome-dependent GTPase activity of EF–Tu was measured by a spectrophotometer (V-550; Jasco) with the GTP-regeneration system (*14*), in which C-terminus (EF–Tu and EF–Ts) and N-terminus (SmpB and AlaRS) His6-tagged proteins were used. Reaction mixtures of 100 μl were pre-incubated at 37°C for 2–3 min in GTPase-buffer [7 mM magnesium acetate, 5 mM potassium phosphate (pH 7.3), 95 mM potassium glutamate, 5 mM ammonium chloride, 0.5 mM calcium chloride, 1 mM spermidine, 8 mM putrescine, 1 mM DTT, 1 mM each of ATP and GTP, 5 mM phosphoenolpyruvate, 0.2 mM NADH, 10 μg/ml pyruvate kinase (Roche), 4 μg L-lactate dehydrogenase (Roche), 100 μM alanine, 1 μg of EF–Ts and 10 μg of AlaRS]. Unless specified, 4 μM EF–Tu, 2 μM SmpB or its variant, and tmRNA (1 μM in Fig. 1C and 2 and 16 nM–2 μM in Fig. 1D) were added to the reaction tubes. Then the ribosomes (0.5μM in Fig. 1, 0.14 μM in Fig. 2) were mixed quickly to initiate GTP hydrolysis reaction. The decrease in absorbance at 340 nm due to the oxidation of NADH was monitored continuously with a spectrophotometer (V550; Jasco). From the slope of the decrease in absorbance at 340 nm, the GTP hydrolysis rates per ribosome were calculated. Using these rates, the biochemical turnover times of EF–Tu were estimated.

SsrA-tagging assay

Tagging ability of fluorescent-labelled tmRNA was examined using samples with 3 Cy5/tmRNA. The DNA template for the truncated DHFR was PCR amplified as described previously (*16*). The reaction condition of the PURE system was as described in previous reports (*17*, *18*). When indicated, 1 μM tmRNA and 2 μM SmpB or its variants were also added to the reaction mixtures. Reactions were started by the addition of 5 μg/ml PCR-amplified DNA template into PURE system solution containing 1.2 μM ribosome, and incubated for 1 h at 37°C. Synthesized proteins containing ^{35}S methionine were separated by 12% of SDS–PAGE and visualized with a BAS-5000 bio-imaging analyzer (Fujifilm).

Preparation of the observation chamber for single molecule imaging

Single molecule imaging was performed in a flow chamber, in which ribosomes were anchored on polyethylene glycol (PEG) coated quartz

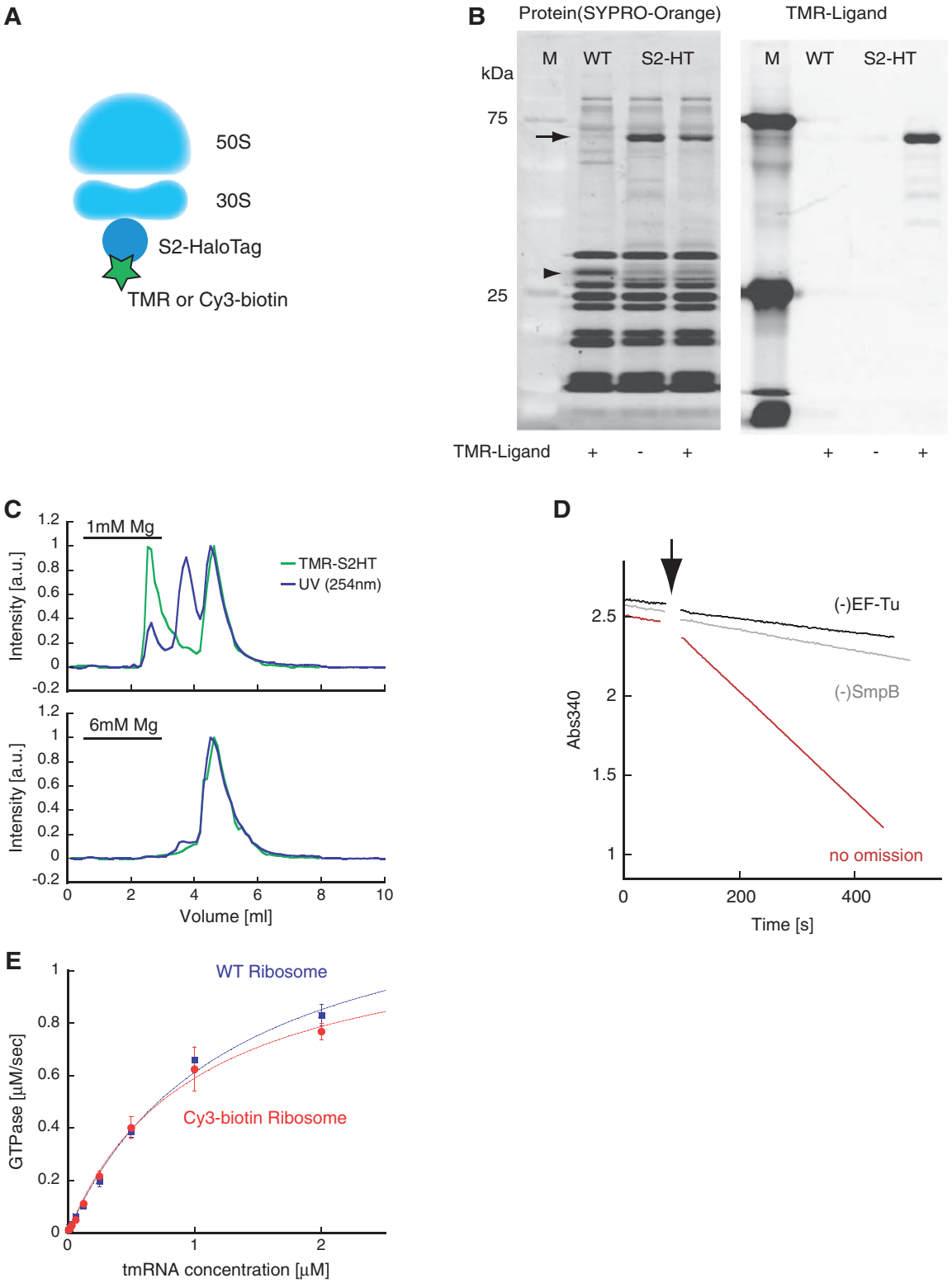

Fig. 1 Fluorescent labelling of ribosomes. (A) Schematic design of fluorescently labelled tagged ribosome. The HaloTag protein was fused to the S2 protein, which is one of the ribosomal proteins of the 30S subunit, and fluorescent dye (TMR in Fig. 1B and C and Cy3–biotin in Figs 1E and 3–5) was covalently labelled using the specific interaction between the HaloTag protein and the HaloTag ligand. (B) Specific labelling of the S2–HaloTag protein (S2–HT) was confirmed by SDS–PAGE. Arrow indicates the position of S2–HT and arrowhead indicates the position of wild-type (WT) S2. (Left) A SYPRO-Orange-stained gel shows the position of the protein band. (Right) A fluorescent image of TMR shows that only S2–HT was labelled with TMR. (C) Incorporation of fluorescently labelled S2–HT into the 30S subunit was confirmed by SDG centrifugation (SDG; 20–50%; 210,000*g* for 7 h). (Upper) At low ionic strength [1 mM $Mg(OAc)_2$], TMR fluorescence was observed at the 30S and 70S positions. (Lower) At normal ionic strength [6 mM $Mg(OAc)_2$], the TMR signal was observed only at the 70S position. (D) The observed GTPase activity requires all ternary components (tmRNA/SmpB/EF–Tu). (E) Fluorescent labelling of S2–HT does not affect the GTPase activity of EF–Tu, showing that the activity of fluorescently labelled ribosome was normal. The V_{max} and K_m values are; WT ribosome: $V_{max} = 1.4\,\mu M/s$, $K_m = 1.3\,\mu M$; Cy3–biotin ribosome: $V_{max} = 1.2\,\mu M/s$, $K_m = 1\,\mu M$.

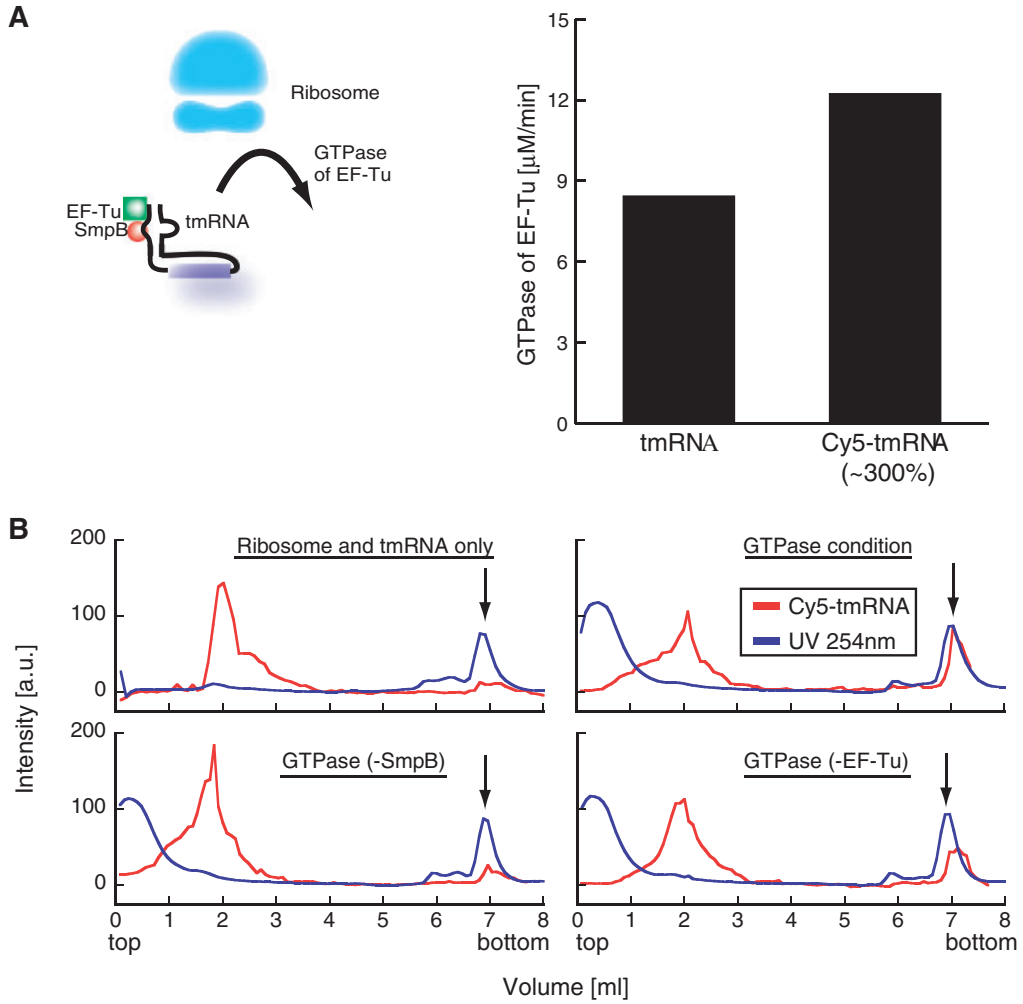

Fig. 2 Fluorescent labelling of tmRNA. (A) Cy5 labelling of tmRNA or tagging of S2 with HaloTag protein does not affect the GTPase activity of EF–Tu. (B) SDG (20–50%; 222,000*g* for 16 h) data shows a specific interaction of Cy5–tmRNA with the ribosome in the GTPase condition (upper right) or in the presence of SmpB (lower right; GTPase condition without EF–Tu). Arrows indicate the position of a ribosome.

slides, and tmRNA/SmpB/EF–Tu and other required materials were infused. PEG coated quartz slides were prepared as previously described (*19*). Briefly, after sonicating quartz slides in 0.1 M KOH, EtOH and MQ water (millipore) for 15 min each, the cleaned quartz slides were amine modified at room temperature for 20 min with 2% (v/v) N-2–(aminoethyl)-3–aminopropyl–triethoxysilane (KBE–603, Shin-Etsu Chemical) in methanol solution containing 135 mM acetic acid and 4% (v/v) MQ water. After washing with MQ water and drying in the clean bench each, quartz slide was PEG coated by dropping of 50 mM MOPS (pH 7.5) buffer containing 10 mg of NHS–PEG (SUNBRIGHT ME-050CS, M.W. = 5,000 Da, NOF) and 0.1 mg NHS–PEG–biotn (Biotin–CONH–PEG–O–C_3H_6–CONHS, 13–5,000–25–35, M.W. = 5,000 Da, Rapp Polymer). A flow chamber of 15 μl volume was made of a PEG coated quartz slide and a non-treated cover glass. To immobilize the ribosomes on the glass slides, 0.33 mg/ml neutra-avidin dissolved in MQ water was infused. After washing with 100 μl of 70S buffer, the uncovered surface was blocked with 1% poly(MPC–co–BMA) (PMB; Biolipidure–203, NOF CORPORATION) in 70S buffer, and then ribosomes in 70S buffer were infused. Excess amounts of PMB and ribosomes were removed by washing with 70S buffer. Finally, the tmRNA/SmpB/EF–Tu ternary complexes in reaction buffer were infused. The final reaction buffer for interaction imaging contained 3 nM Cy5–tmRNA, 2 μM SmpB, 4 μM EF–Tu, 100 nM 50S ribosomal subunit and an O_2 scavenger system (50 U/ml glucose–oxidase (G2133, Sigma), 50 U/ml catalase (C40, Sigma), 4.5 mg/ml glucose and 10 mM DTT) in GTPase buffer. The final reaction buffer was pre-incubated for 5 min at 37°C before being infused into the flow chamber.

Imaging and analysis

Single molecule images were visualized by a total internal reflection fluorescence microscope equipped on an inverted type microscope (IX70; Olympus), as previously described (*20–22*). The Cy3 and Cy5 dyes were illuminated with an argon laser (514 nm; 35LAP321, Melles Griot) and a He-Ne laser (633 nm; 31-2082-000, Coherent), respectively. In Fig. 3, both green and red lasers were used simultaneously to evaluate non-specific binding of the tmRNA/SmpB/EF–Tu ternary complex to the glass surface. To observe the binding and unbinding events of the tmRNA/SmpB/EF–Tu ternary complex onto and from the anchored ribosome as illustrated in Fig. 5, images were taken with red laser excitation for 5 min. To visualize the ribosome position, a green laser was used at the first and last 5 s of the 5 min observation. Fluorescence images from Cy3 and Cy5 were separated by using a Dual-View (Optical Insights) and then projected side-by-side onto an electron-multiplying charge coupled device camera (iXon DV860 DCS-BV; Andor). Images were taken at a frame rate of 10 frames/s, and the observations were carried out at 24 ± 1°C. Images were analysed using Image J software (http://rsb.info.nih.gov/ij/) with a built-in function and custom-designed plug-in software. The fluorescent intensity of the spots was measured using 6 pixel diameter circular ROIs (regions of interest). The background values were then subtracted from the obtained values and analysed. To analyse the duration of the interaction, data were fitted by a non-linear least squares fitting of the cumulative probability distribution [C1*(1 – C2*exp (–t/C3) – (1 – C2)*exp (–t/C4)) – C5], where C1 is a normalized parameter, C2 is a fraction parameter for fast components, C3 is the dwell time for fast components and C4 is the dwell time for slow components. C5 was used to exclude the

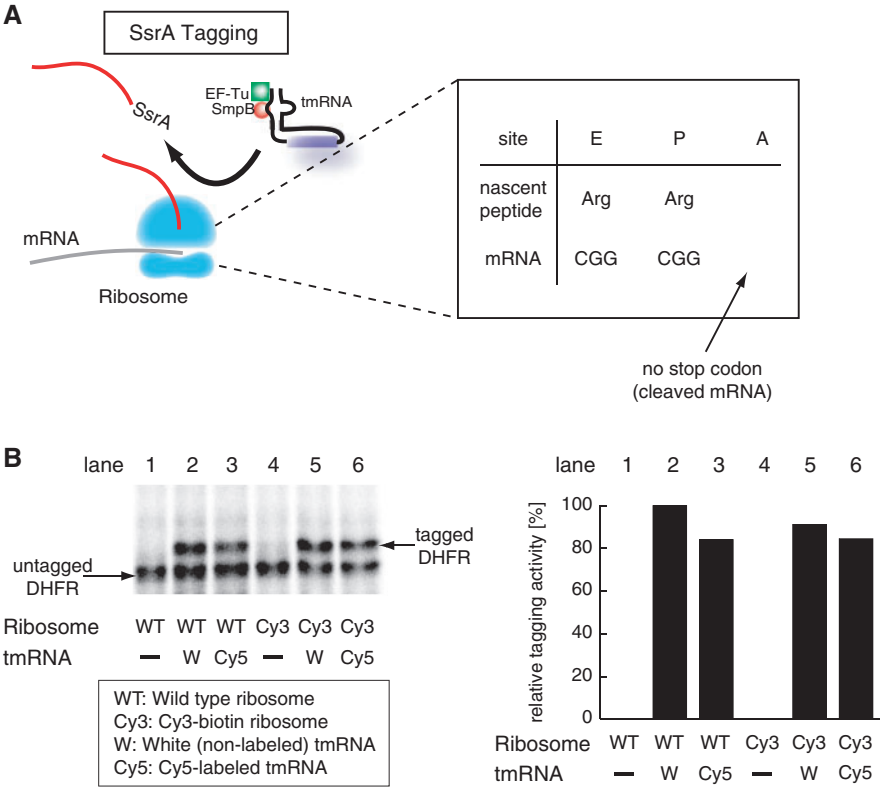

Fig. 3 SsrA-tagging assay in PURE system. (A) A Schematic diagram illustrating the SsrA-tagging experiment. Truncated DHFR nascent peptide was used as a model stalled nascent peptide. (B) Addition of 11 amino acids to the stalled nascent peptide was confirmed by SDS–PAGE (left) and quantified by measuring the intensity of tagged DHFR band of each lane [right bar graph; data of WT non-labelled ribosome and white (non-labelled) tmRNA (lane 2) was set to 100%, showing that the SsrA-tagging activity of Cy3–biotin–Ribosome and Cy5–tmRNA were normal.

effect of the counting loss. To avoid the photo bleaching effect of the fluorophore, the obtained dwell time (*i.e.* C3 or C4) was corrected as reported (*23*) by using the following equation:

$$k_{\text{obtained}} = k_{\text{corrected}} + k_{\text{bleach}} \quad (1)$$

where, k_{obtained} is the inverse of obtained dwell time (*i.e.* 1/C3 or 1/C4), $k_{\text{corrected}}$ is the corrected actual rate constant (inverse of the required actual dwell time) and k_{bleach} is the measured photo bleaching rate of the fluorophore at the observation condition.

Results and Discussion

Fluorescent labelling of ribosomes

For anchoring of ribosomes onto glass slides, we constructed protein-tagged ribosomes (Fig. 1A). Ribosomal protein S2 of the 30S subunit was fused to the HaloTag protein and ribosomes were purified as described (*11*). The yield of modified ribosomes from *E. coli* was similar to that of wild-type ribosomes, which enabled us to perform bulk biochemical experiments routinely. Furthermore, the rapid (k_{on} is near 10^7/M/s according to the manufacturer) and specific labelling of the HaloTag ligand to the HaloTag protein allowed us to obtain uniform and highly labelled ribosomes. To prepare fluorescently labelled ribosomes, we mixed fluorescently labelled HaloTag ligand (TMR ligand) with ribosomes at a ribosome to TMR ligand molar ratio of 1 : 4 and reacted for 30 min at room temperature. After a short gel filtration step using spin column centrifugation (1 min), we obtained a sufficient amount of labelled ribosomes at a label ratio of 0.9 TMR dye/ribosome. In contrast, non-tagged wild-type ribosomes were hardly labelled with this procedure (<0.01 TMR/ribosome). Specific labelling of the HaloTag protein fused S2 ribosomal protein (S2–HT) was confirmed by SDS–PAGE (Fig. 1B). SDG experiments also showed the incorporation of fluorescently labelled S2–HT into the 30S subunit (Fig. 1C). These results show the specific and stable labelling of tagged ribosomes by a fluorescent dye.

Next, we prepared the ribosomes simultaneously labelled with the multi-functional HaloTag ligand including Cy3 dye and biotin moieties. We chemically conjugated Cy3 and biotin to HaloTag ligand as described (*12*, *13*), and specific ribosome labelling of Cy3 and biotin were confirmed by SDS–PAGE and biotin detection kit (data not shown).

The activity of Cy3–biotin-labelled ribosomes was confirmed by measuring the GTPase activity of EF–Tu at the entry process of *trans*-translation. At the entry process of the *trans*-translation process, tmRNA enters the A site of the stalled ribosome in an alanine-charged form with the aid of SmpB and EF–Tu. As this entry process is highly dependent on the presence of each component (*14*), any defect in the function of the ribosome should decrease the GTPase activity of the EF–Tu. Actually, the GTPase of EF–Tu using fluorescently labelled ribosomes was similar to that of wild-type non-labelled ribosomes (Fig. 1D and E). Furthermore, we evaluated the

translation activity of fluorescently labelled ribosomes by an *in vitro* translation system [the PURE system (*17*)]; using GFP protein as the model template. The activity of the labelled ribosome was 70% of that of wild-type ribosomes (data not shown). These results show that the activity of the labelled ribosomes was similar to that of wild-type ribosomes.

Fluorescent labelling of tmRNA

tmRNA is a 365 nt RNA and has a conserved TLD, four pseudoknots and an MLD. First, we attempted to label the tmRNA at the 5′-end by introducing a reactive group (*10*), but the labelling efficiency of this method was low (<25%). Therefore, we took another labelling approach. We chose to randomly label guanine residues. With this method, we were able to control the labelling efficiency by changing either the molar ratio of dye to tmRNA or the reaction time.

Fluorescent labelling of tmRNA had little effect on the GTPase activity of EF–Tu at the entry process of *trans*-translation (Fig. 2A). SDG experiments confirmed the specific interaction of Cy5–tmRNA to ribosomes, for which SmpB and EF–Tu are required (Fig. 2B). Furthermore, SsrA-tagging ability (add 11 amino acids long degradation tag peptide to the nascent stalled peptide) was similar level compared with the non-labelled tmRNA (Fig. 3).

Specific interaction between anchored ribosomes and the tmRNA/SmpB/EF–Tu ternary complex

In single molecule imaging, blocking of non-specific binding of the target molecule to the glass surface is crucial. To evaluate the non-specific binding of Cy5–tmRNA, we first infused the Cy5–tmRNA/SmpB/EF–Tu ternary complex into the flow chamber without anchoring the ribosomes. But the PEG coated quartz slides could not prevent non-specific binding of the Cy5–tmRNA/SmpB/EF–Tu ternary complex to the glass surface (Fig. 4A, left). With an extensive survey, we found that treatment of the flow chamber with 1% poly [2-methacryloyloxyethyl phosphorylcholine (MPC)–co–*n*-butyl methacrylate (BMA)] (hereafter, 'PMB') could significantly reduce non-specific binding of the Cy5–tmRNA/SmpB/EF–Tu ternary complex to the glass surface (Fig. 4A, right).

Next, we checked the specific interaction of Cy5–tmRNA/SmpB/EF–Tu onto the anchored ribosome. First, Cy3–biotin–ribosomes were anchored on glass surface through biotin–avidin interaction. The number of observed Cy3–biotin–ribosome spots depended on the concentration of infused Cy3–biotin–ribosome (Fig. 4A, right and Fig. 4B, left). Furthermore, when neutra-avidin infusion step was omitted from the chamber preparation procedure, no fluorescent spots were observed in Cy3–channel (data not shown). These results indicate specific binding of the Cy3–biotin–ribosome onto the glass surface through biotin–avidin interaction.

After anchoring of Cy3–biotin–ribosome on glass surface, Cy5–tmRNA/SmpB/EF–Tu ternary complex was infused into the observation chamber. The number of observed fluorescent spots depended on the concentration of infused ribosomes, indicating specific binding of the Cy5–tmRNA/SmpB/EF–Tu ternary

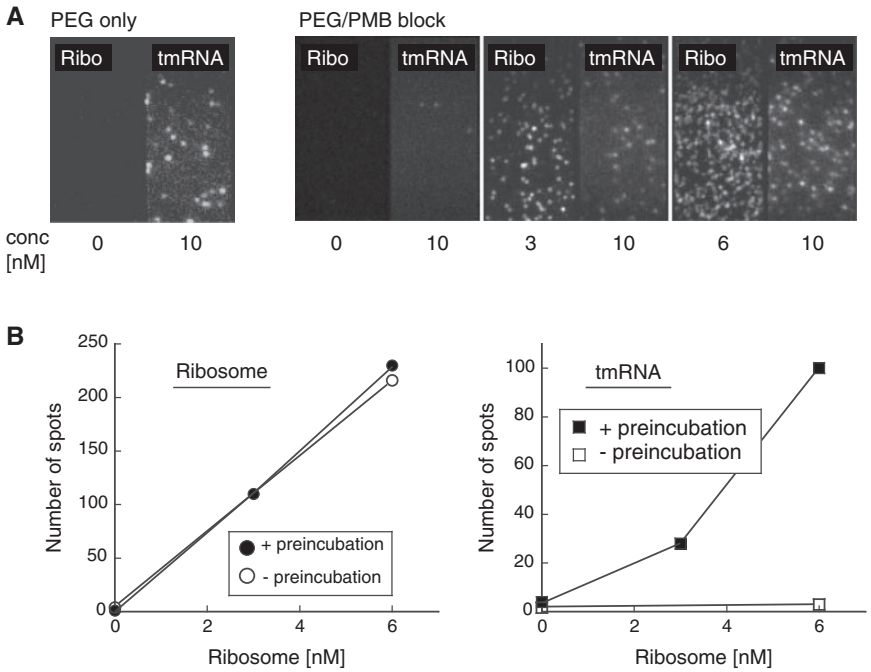

Fig. 4 Specific interaction between anchored ribosomes and the tmRNA/SmpB/EF-Tu ternary complex. (A) Blocking of non-specific Cy5–tmRNA binding to the glass surface. The left and right sides of the image show the Cy3–ribosome and Cy5–tmRNA, respectively. (Left) PEG coated quartz slides are unable to block the non-specific Cy5–tmRNA binding to the glass surface completely. (Right) Blocking of the uncovered surface with 1% PMB effectively reduces non-specific Cy5–tmRNA binding. Furthermore, the number of Cy5–tmRNA spots depend on the concentration of anchored Cy3–ribosomes. (B) Pre-incubation (37°C, 5 min) of the Cy5–tmRNA/SmpB/EF–Tu ternary complex increased the number of associated Cy5–tmRNA spots. Taken together with the similar effect of the pre-incubation on GTPase at 25°C (Supplementary Fig. S1), we concluded that pre-incubation is critical for the specific interaction of the Cy5–tmRNA/SmpB/EF–Tu ternary complex with the ribosome.

complex onto the ribosome. Furthermore, for imaging at room temperature (24 ± 1°C), pre-incubation of the Cy5–tmRNA/SmpB/EF–Tu ternary complex at 37°C for 5 min was required to obtain a sufficient number of interactions (Fig. 4B, right). Pre-incubation at 37°C might promote the active complex formation. Without pre-incubation at 37°C, aggregated blight spots of Cy5–tmRNA, which may indicate the inefficient formation of active complex, were also observed under microscope. But after pre-incubation at 37°C for 5 min, these aggregated blight spots disappeared. Taking these results together with the similar effect of pre-incubation on GTPase at 25°C (Supplementary Fig. S1), we concluded that pre-incubation is critical for the specific interaction of the Cy5–tmRNA/SmpB/EF–Tu ternary complex onto ribosomes at room temperature. These data show that the fluorescent spots observed represent the Cy5–tmRNA/SmpB/EF–Tu ternary complex bound specifically to anchored ribosomes.

Single molecule imaging of the entry process of trans*-translation*

To elucidate the *trans*-translation entry process, we observed the interaction of the Cy5–tmRNA/SmpB/EF–tu ternary complex onto anchored ribosomes (Fig. 5A). Under our observation conditions, where the stalled mRNA and the stalled nascent peptide were lacking, the ribosome associated tmRNA/SmpB/EF–Tu ternary complex could not proceed to the following processes, such as the transfer of alanine to the nascent peptide and SsrA tagging (translation using the ORF of tmRNA) of the nascent peptide. Thus, after a short period of interaction, the process would be aborted and tmRNA/SmpB/EF–Tu might leave from the ribosome and another round of interactions would resume. Indeed, the GTPase activity of EF–Tu indicates continuous interaction during the measurements (Fig. 1D), which supports this hypothesis. For these reasons, multiple rounds of interaction of the tmRNA/SmpB/EF–Tu ternary complex with anchored ribosomes may be expected during single molecule imaging. On simultaneous excitation with the green and red lasers, discrete fluorescent spots were observed both in the Cy3 (ribosome) channel and in the Cy5 (tmRNA) channel. The discrete fluorescent spots corresponding to Cy5–tmRNA appeared and disappeared from the image, suggesting that multiple rounds of interaction occurred as expected (Fig. 5B).

The fluorescence intensities of Cy3–ribosome and Cy5–tmRNA were the same as those of a single fluorophore as expected from the label efficiency (Supplementary Fig. S2). From these results, we concluded that most of the observed interactions were those of single ternary complexes of tmRNA/SmpB/EF–Tu with single ribosomes.

At 10 nM concentration, the Cy5–tmRNA/SmpB/EF–Tu ternary complex bind with a rate constant of $0.026\,s^{-1}$ [second-order rate constant of 2.6×10^6 (1/M/s)]; calculated from the histogram of the 'off-time' for the binding (*i.e.* the duration of the off period); (Supplementary Fig. S3). This value is an order of magnitude lower than the reported value for bulk experiment using tRNA/GTP/EF–Tu complex [6×10^7 (1/M/s)]; (*24*). Following two factors might affect the association rate constant. First, different structure of tmRNA (lacking anticodon and D loop) compared with tRNA might cause the difference in affinity to the ribosome. Second, the steric and surface effects might affect the association rates as reported for tRNA/GTP/EF–Tu interaction to glass surface immobilized ribosome (*7*). Further studies are required to resolve this point.

Next, the duration of individual events was analysed (Fig. 5C). With single molecule imaging, the obtained data are not obscured by ensemble averaging. Therefore, it is expected that one can easily distinguish whether the interaction is composed of single process or multiple processes. To resolve this point, we fitted the data with single or the sum of two exponential functions. The data fitted well with the sum of two exponential functions rather than with the single exponential function (Supplementary Fig. S4), implying the existence of a multi-modal interaction. To further confirm that the interaction was specific, we performed a series of control experiments. First, we omitted SmpB from the reaction solution. The GTPase (data not shown) and SDG experiments (Fig. 2B, left side of lower panel) indicate a reduced interaction between tmRNAs and ribosomes. Observing this condition under a microscope, we found fewer ribosomal interactions for Cy5–tmRNA (0.18 events/ribosome/min) compared with the normal ternary complex (tmRNA/SmpB/EF–Tu: 1.0 events/ribosome/min), as expected (Fig. 5C). Second, we removed EF–Tu from the reaction solution to assess GTPase independent binding of the tmRNA/SmpB complex on ribosome. But using this condition, we found that non-specific binding of Cy5–tmRNA to the glass surface was severe. Thus, rather than removing EF–Tu from the reaction solution, we used a GTPase defective mutant (G222D) (*25*). Using this condition, the SDG data indicated a weak interaction between tmRNA and the ribosome [data not shown, but see Fig. 2B, right side of lower panel (labelled 'condition of EF–Tu' in the figure)]. As expected, we found a lower frequency of Cy5–tmRNA interactions with ribosomes (Fig. 5C, middle: 0.45 events/ribosome/min). From these results, we conclude that approximately half of the observed fluorescent spots correspond to GTPase dependent interaction of tmRNA/SmpB/EF–Tu ternary complexes.

To resolve the GTPase dependent interaction further, we examined precisely the duration of interaction. For all conditions, most of the interactions were short [the 'Cy5 photo bleaching effect'-corrected durations τ were in the range of 0.92–1.2 s; (Table I)], and these interaction times were equivalent to the turnover time of EF–Tu estimated from biochemical GTPase experiments (0.9 s; Fig. 2A). But the fraction of longer duration interactions (corrected duration τ was 25 s) increased when using tmRNA/SmpB/EF–Tu. To assess the fraction to which GTPase contributed, we subtracted G222D data from that of the normal tmRNA/SmpB/EF–Tu ternary complex

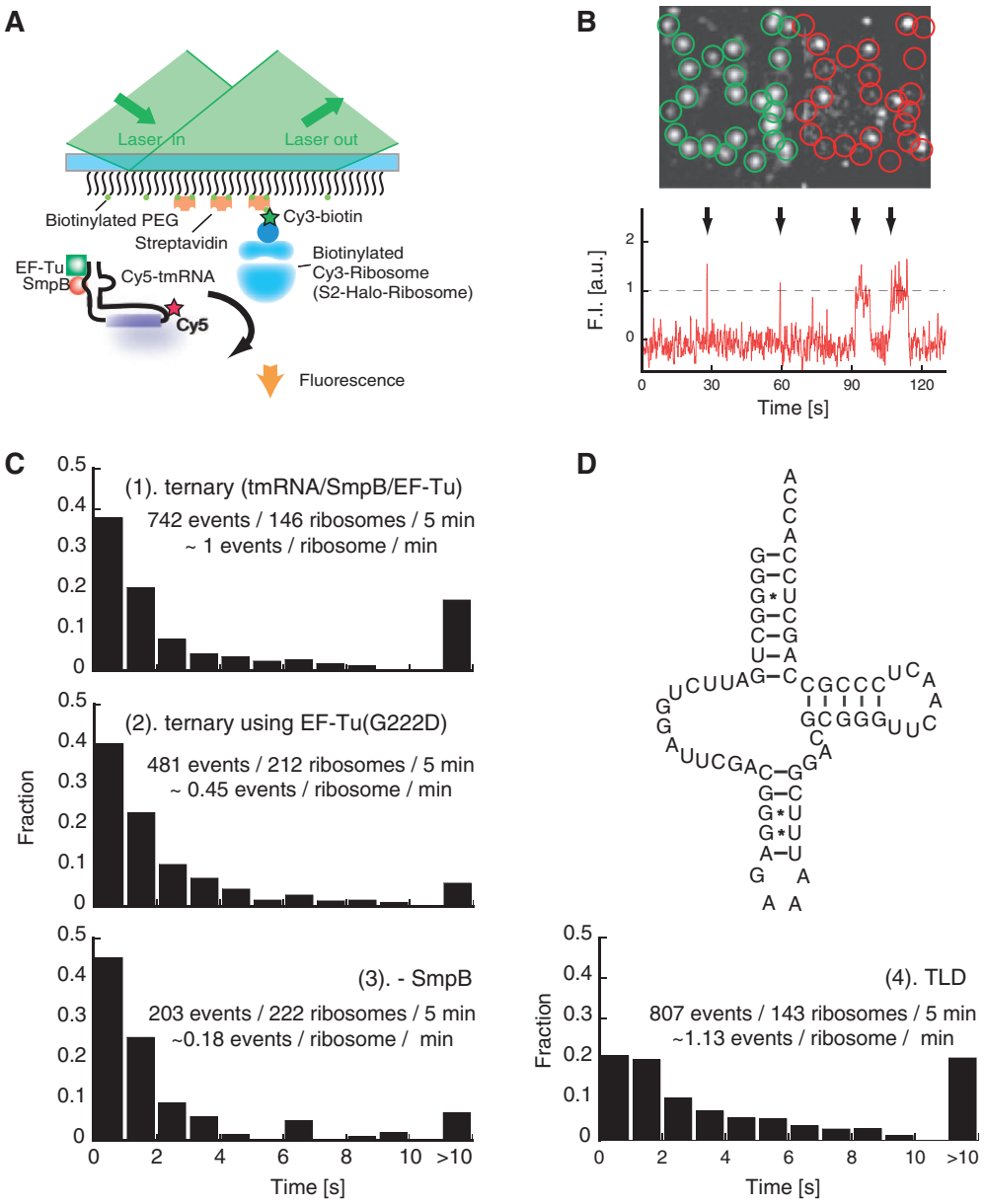

Fig. 5 Single molecule imaging of the entry process of trans-translation. (A) A schematic diagram illustrating single molecule imaging of the entry process of *trans*-translation. (B) (Upper) A typical single molecule measurements image. The position of Cy3–ribosomes is shown as circle ROI in both Cy3 (ribosome) and Cy5 (tmRNA) channel. (Lower) A typical trace of the fluorescent intensity of Cy5–tmRNA associating and dissociating with the single ribosome. Arrows indicate the position of interaction. The dashed line drawn at fluorescent intensity 1 indicates the threshold line to detect the interaction. (C) A histogram of 'attachment time' shows the interaction of Cy5–tmRNA under several experimental conditions, in which horizontal axis is the duration of attachment time (duration of 'on' in Supplementary Fig. 3A), and vertical axis is the fraction of each bin calculated by dividing 'the number of events of each bin' by 'total event numbers (*e.g.* 742 in the upper graph)'. The estimated kinetic parameters are presented in Table I. Note: the slow fraction (the obtained (not corrected) durations τ were in the range of 5.3–7.1 s) of the data shown in Fig. 5 was much affected by photo bleaching of Cy5 (10 s for the data presented in Fig. 5). To avoid the photo bleaching effect, we corrected the obtained data using the reported method (*23*). Furthermore, similar corrected data were obtained under the low laser power conditions (Supplementary Fig. S4B). (D) To assess the contribution of tmRNA unique structure (*e.g.* MLD and four pseudoknots) we measured only the construct TLD. Similar kinetic parameters to tmRNA were obtained indicating that the existence of MLD and/or four pseudoknots is not the reason of tmRNA multiple pathway interaction.

(Supplementary Fig. S5). Both the short and long duration fractions remained, indicating that multiple pathways exist during GTPase production. As the duration of the interactions of the fast components is similar to that of the bulk biochemical experiments, this fraction might reflect a simultaneous attachment and detachment of the tmRNA/SmpB/EF–Tu ternary complex. In contrast, the duration of the interactions of the slow components was much longer than that estimated from bulk experiments. This might reflect the asynchronous interaction of tmRNA/SmpB and EF–Tu. One possibility is that EF–Tu drops off from the ribosome–tmRNA/SmpB/EF–Tu complex. If this is the case, we would expect an asynchronous interaction of EF–Tu and tmRNA, as well as multiple rounds of associations of EF–Tu to the

Table I. Kinetic parameters estimated by fitting the data with the sum of two exponential functions.

	Fast		Slow	
Condition	**Fraction**	**τ [s]**	**Fraction**	**τ [s]**
wt (tmRNA/SmpB/EF–Tu)	0.61	0.94	0.39	25
G222D [tmRNA/SmpB/EF–Tu(G222D)]	0.68	1.2	0.32	11
SmpB (tmRNA/EF–TU)	0.8	0.92	0.2	25
TLD (TLD/SmpB/EF–Tu)	0.48	1.5	0.52	20

The kinetic parameters were corrected using the reported method (*23*) to avoid the effect of Cy5 photo bleaching. The obtained (not corrected) duration τ of fast and slow fractions were in the range of 0.84–1.3 s and 5.3–7.1 s, respectively.

ribosome–tmRNA/SmpB complex, resulting in the continuous GTPase activity produced by EF–Tu while tmRNA remains attached to the ribosome. We also examine whether the unique structure of tmRNA affect the multiple pathway interaction. To do this, we truncated MLD and four pseudoknots from tmRNA, thus the resulting construct has only TLD (Fig. 5D). Similar kinetic parameters to tmRNA were obtained indicating that the existence of MLD and/or four pseudoknots is not the reason of tmRNA multiple pathway interaction. A future study that includes simultaneous imaging of EF–Tu or SmpB with tmRNA is required to resolve this uncertain point.

In summary, we have developed a new method to image the entry process of *trans*-translation at the single molecule level using anchored ribosomes. Combining with recent real-time imaging of tRNA interaction on translating ribosome (*3*, *4*, *7*), our method was able to resolve the whole mechanism of *trans*-translation. Furthermore, our method in which ribosomes are covalently labelled with chemical moiety conjugated HaloTag ligand provides a sufficient amount of specific and stably labelled ribosomes. This strategy might be useful for elucidating the translation mechanism *in vitro* and *in vivo*.

Supplementary Data

Supplementary Data are available at *JB* Online.

Acknowledgements

We thank Y Miyazono for reading the article and for useful comments.

Funding

City Area Program (to T.U.); The Ministry of Education, Culture, Sports, Science and Technology of Japan, grant-in-aid for Scientific Research on Priority (17026008 to T.U., 19058002 to H. Taguchi); grants-in-aid (17310123 to K.I., 22570156 to H. Tadakuma); grants-in-Aid for Young Scientists (19770143 to Y.S.).

Conflict of interest

None declared.

References

1. Haebel, P.W., Gutmann, S., and Ban, N. (2004) Dial tm for rescue: tmRNA engages ribosomes stalled on defective mRNAs. *Curr. Opin. Struct. Biol.* **14**, 58–65
2. Keiler, K.C. (2008) Biology of trans-translation. *Annu. Rev. Microbiol.* **62**, 133–151
3. Blanchard, S.C., Kim, H.D., Gonzalez, R.L. Jr, Puglisi, J.D., and Chu, S. (2004) tRNA dynamics on the ribosome during translation. *Proc. Natl. Acad. Sci. USA* **101**, 12893–12898
4. Blanchard, S.C., Gonzalez, R.L. Jr, Kim, H.D., Chu, S., and Puglisi, J.D. (2004) tRNA selection and kinetic proofreading in translation. *Nature Struct. Mol. Biol.* **11**, 1008–1014
5. Cornish, P.V., Ermolenko, D.N., Noller, H.F., and Ha, T. (2008) Spontaneous intersubunit rotation in single ribosomes. *Mol. Cell* **30**, 578–588
6. Fei, J., Kosuri, P., MacDougall, D.D., and Gonzalez, R.L. Jr. (2008) Coupling of ribosomal L1 stalk and tRNA dynamics during translation elongation. *Mol. Cell* **30**, 348–359
7. Uemura, S., Aitken, C.E., Korlach, J., Flusberg, B.A., Turner, S.W., and Puglisi, J.D. (2010) Real-time tRNA transit on single translating ribosomes at codon resolution. *Nature* **464**, 1012–1017
8. Dorywalska, M., Blanchard, S.C., Gonzalez, R.L. Jr, Kim, H.D., Chu, S., and Puglisi, J.D. (2005) Site-specific labeling of the ribosome for single-molecule spectroscopy. *Nucleic Acids Res.* **33**, 182–189
9. Uemura, S., Iizuka, R., Ueno, T., Shimizu, Y., Taguchi, H., Ueda, T., Puglisi, J.D., and Funatsu, T. (2008) Single-molecule imaging of full protein synthesis by immobilized ribosomes. *Nucleic Acids Res.* **36**, e70
10. Stapulionis, R., Wang, Y., Dempsey, G.T., Khudaravalli, R., Nielsen, K.M., Cooperman, B.S., Goldman, Y.E., and Knudsen, C.R. (2008) Fast in vitro translation system immobilized on a surface via specific biotinylation of the ribosome. *Biol. Chem.* **389**, 1239–1249
11. Ohashi, H., Shimizu, Y., Ying, B.W., and Ueda, T. (2007) Efficient protein selection based on ribosome display system with purified components. *Biochem. Biophys. Res. Commun.* **352**, 270–276
12. Conley, N.R., Biteen, J.S., and Moerner, W.E. (2008) Cy3-Cy5 covalent heterodimers for single-molecule photoswitching. *J. Phys. Chem. B.* **112**, 11878–11880
13. Huang, B., Jones, S.A., Brandenburg, B., and Zhuang, X. (2008) Whole-cell 3D STORM reveals interactions between cellular structures with nanometer-scale resolution. *Nat. Methods* **5**, 1047–1052
14. Shimizu, Y. and Ueda, T. (2006) SmpB triggers GTP hydrolysis of elongation factor Tu on ribosomes by compensating for the lack of codon-anticodon interaction during trans-translation initiation. *J. Biol. Chem.* **281**, 15987–15996
15. Tadakuma, H., Ishihama, Y., Shibuya, T., Tani, T., and Funatsu, T. (2006) Imaging of single mRNA molecules moving within a living cell nucleus. *Biochem. Biophys. Res. Commun.* **344**, 772–779
16. Qi, H., Shimizu, Y., and Ueda, T. (2007) Ribosomal protein S1 is not essential for the trans-translation machinery. *J. Mol. Biol.* **368**, 845–852
17. Shimizu, Y., Inoue, A., Tomari, Y., Suzuki, T., Yokogawa, T., Nishikawa, K., and Ueda, T. (2001) Cell-free translation reconstituted with purified components. *Nat. Biotechnol.* **19**, 751–755
18. Shimizu, Y., Kanamori, T., and Ueda, T. (2005) Protein synthesis by pure translation systems. *Methods* **36**, 299–304

19. Yokota, H., Han, Y.W., Allemand, J.-F., Xi, X.G., Bensimon, D., Croquette, V., Ito, Y., and Harada, Y. (2009) Single-molecule Visualization of Binding Modes of Helicase to DNA on PEGylated Surfaces. *Chem. Lett.* **38**, 308–309
20. Funatsu, T., Harad, Y., Tokunaga, M., Saito, K., and Yanagida, T. (1995) Imaging of single fluorescent molecules and individual ATP turnovers by single myosin molecules in aqueous solution. *Nature* **374**, 555–559
21. Taguchi, H., Ueno, T., Tadakuma, H., Yoshida, M., and Funatsu, T. (2001) Single-molecule observation of protein-protein interactions in the chaperonin system. *Nat. Biotechnol.* **19**, 861–865
22. Miyazono, Y., Hayashi, M., Karagiannis, P., Harada, Y., and Tadakuma, H. (2010) Strain through the neck linker ensures processive runs: a DNA-kinesin hybrid nanomachine study. *EMBO J.* **29**, 93–106
23. Romberg, L., Pierce, D.W., and Vale, R.D. (1998) Role of the kinesin neck region in processive microtubule-based motility. *J. Cell Biol.* **140**, 1407–1416
24. Pape, T., Wintermeyer, W., and Rodnina, M.V. (1998) Complete kinetic mechanism of elongation factor Tu-dependent binding of aminoacyl-tRNA to the A site of the E. coli ribosome. *EMBO J.* **17**, 7490–7497
25. Vorstenbosch, E., Pape, T., Rodnina, M.V., Kraa, l B., and Wintermeyer, W. (1996) The G222D mutation in elongation factor Tu inhibits the codon-induced conformational changes leading to GTPase activation on the ribosome. *EMBO J.* **15**, 6766–6774